This is a preprint version of the article: S. R. Nekoo, and A. Ollero, “A Robust State-Dependent Riccati Equation Controller with Parameter Uncertainty and Matched Disturbance,” Journal of the Franklin Institute, 2023. https://doi.org/10.1016/j.jfranklin.2023.11.023

Highlights

A Robust State-Dependent Riccati Equation Controller with Parameter Uncertainty and Matched Disturbance

Saeed Rafee Nekoo, Anibal Ollero

- A robust SDRE design is proposed based on the defined bound of the uncertainty in the weighting matrices.
- The stability of the controller is proved using the Lyapunov method to find the weighting matrices.
- A fourth-order nonlinear system is simulated as an example of the proposed method.

A Robust State-Dependent Riccati Equation Controller with Parameter Uncertainty and Matched Disturbance

Saeed Rafee Nekoo[a], Anibal Ollero[a,b]

[a] *The GRVC Robotics Lab., Departamento de Ingeniería de Sistemas y Automática, Escuela Técnica Superior de Ingeniería, Universidad de Sevilla, Seville, 41092, Spain*
[b] *FADA-CATEC, Centro Avanzado de Tecnologías Aeroespaciales, Seville, 41300, Spain*

Abstract

The state-dependent Riccati equation (SDRE) unveils a nonlinear optimal control approach; the method is sensitive to uncertainty and disturbance that provokes the necessity of precise modeling and omitting disturbance from the model and environment which is occasionally impossible. In this paper, a robust state-dependent Riccati equation is introduced using only the pure SDRE itself. Lyapunov's second method for stability analysis is used to extract two tuning rules for weighting matrices of the robust approach for handling both matched disturbance and parametric uncertainty. A fourth-order differential equation is simulated to show the effectiveness of the suggested method and the results were compared with conventional SDRE. The robust version could handle the matched disturbance with a steady-state shift from the equilibrium point where the conventional SDRE failed. Additionally, a comparison and detailed analysis have been performed between the proposed design and sliding mode control.

Keywords: SDRE, Robust, Nonlinear, Optimal, Closed-loop, Matched uncertainty.

1. Introduction

The state-dependent Riccati equation (SDRE) is an optimal nonlinear controller (closed-loop), proposed by Pearson in the 1960s [1]. The structure of the method mimics the linear quadratic regulator; however, there exists nonlinearity in the system and weighting matrices [2]. Optimality, systematic solution, and flexibility in design were reported as the benefits of this approach [3]. The systematic solution refers to the routine procedure of

the SDRE after the definition of state-dependent coefficient (SDC) parameterization matrices, $\{\mathbf{A}(\mathbf{x}(t)), \mathbf{B}(\mathbf{x}(t))\}$; which include the dynamics of the system in question. Arranging the SDC matrices, one could solve the Riccati equation and find the suboptimal gain of the controller. A part of flexibility in design is gained by non-unique state-dependent coefficient parameterization of the system matrices, recalled as "additional degrees of freedom" [4]. The second part of flexibility could be referred to as an easy combination of the SDRE with other techniques, such as fuzzy [5, 6], sliding mode control (SMC) [7, 8], neural network [9, 10], etc. The motivation for combining the SDRE with other methods is to enhance the performance including speed of regulation, better tuning, finding an adaptive structure, robustness, etc. A pure traditional SDRE controller is quite sensitive to model uncertainty; any deviation in the model from real dynamic increases the error. The sliding mode control has been one of the best options to add robust characteristics to the SDRE [11]. Additionally, the robustness could be gained by a combination of the SDRE and H_∞ approach [12, 13]. Obtaining robustness through function approximation [14], impedance control [15], integral sliding mode [16, 17], etc. could be done successfully; however, the question is how to present a robust SDRE method by using only the method itself. This could be an advantage to present an independent robust-SDRE and keep the robust design under the umbrella of the SDRE without using other methods or combinations with supplementary tools such as neural networks or fuzzy approach. A unified design simplifies the implementation and tuning significantly.

Disturbance and parameter uncertainty could affect the entire state-space system which could be referred to as mismatched uncertainty, or they could only occur in the order of differentiation, referred to as matched disturbance and uncertainty. Sliding mode control is an effective method that could handle both matched and mismatched uncertainty [18]. Wang et al. presented an adaptive SMC for persistent dwell-time switched nonlinear systems with matched/mismatched uncertainties [19]. Kim and Kwon investigated robust stabilization for a balancing robot, rolling on an unleveled terrain [20]. They proposed a disturbance compensation method for the under-actuated system and verified the approach experimentally. Nonsingular terminal sliding mode control was used for controlling a system with matched uncertainty and applied for wheeled mobile robot control [21]. Robust structures for SDRE were defined using additional terms in the weighting matrix of states [14, 22, 23]. Introducing the robust terms in the cost function and weighting matrix was

done to enhance the control law based on updated matrices. Kuo studied chaos synchronization using robust SDRE by adding terms to the weighting matrix and cost function as well for matched and mismatched cases; the size of the input vector was increased to incorporate the robust terms of the performance index in the augmented state-space equation [24]. This idea was also extended to more general cases and applications such as flexible joint arms [14, 23].

Robust optimal control uses a combination of methods to present effective structures. Dung et al. employed an event-triggered approach to handle external disturbance for mobile robots [25]. A combination of adaptive dynamic programming, zero-sum game theory, and an event-triggered mechanism was used to optimize an H_∞ cost function. Xiong and Liu studied robust and optimal control via a barrier penalty function method for fixed-wing platforms in low-attitude trajectories [26]. Qiu et al. researched an observer-based robust optimal control with uncertainty and disturbance [27]. The case study used the attitude and altitude dynamics of a helicopter. Yang et al. presented a robust adaptive control design to handle uncertainty and unmatched disturbances [28]. The control mechanism started the process by estimating nonlinearly parametrized system dynamics and designed an adaptive parameter estimation algorithm and a robust adaptive control design for handling unmatched disturbances, that guaranteed the global boundedness. The adaptive robust design was also implemented on an air vehicle with partial nonlinear parameterizations [29]. The mentioned works used an adaptive mechanism and estimation to incorporate a proper signal for the uncertain part of the dynamics. The similarity of the proposed robust SDRE is that the adaptive robust mechanism is inside the weighting matrix of the states, derived from the Lyapunov method. The highlighted difference between the robust adaptive controllers and the robust SDRE could be seen in the unified compact derivation of the method in this work which could imply the simplicity of the implementation for practical works.

In this work, the system is not augmented and the same number of inputs will be considered in comparison with [14, 23, 24], and also the Lyapunov function will be used to find the modified state and input matrices for robust design. The Lyapunov function was used to show stability in [22], though here in this work, it will set the robust tuning in addition to that; the parameter uncertainty is mismatched and the disturbance is matched. The trade-off between additional complexity versus better performance has been always discussed while presenting an increment contribution to available methods.

Original methods, such as SDRE in this case, present the basis of the control design with simple steps and results in a fair performance. However, their framework is defined within a limited range of systems and conditions, i.e. systems without uncertainty or disturbance, ones with zero equilibrium point, etc. Development of the new branches and versions from conventional SDRE and the combination of that with other techniques enhance the performance at the cost of more computational burden, complexity, and extra machinery. Here the intention is to use the potential of the SDRE and present two simple tuning rules based on the second Lyapunov stability criteria to solve one of the most important issues of the SDRE, which is the lack of robustness in terms of uncertainty in modeling.

The main contributions of this work are as follows. 1) Introducing a robust state-dependent Riccati equation via the nonlinear structure of the weighting matrices of the method itself, without input augmentation nor combination with other methods. 2) Using the Lyapunov function for guaranteeing stability, two conditions have been generated for adding robustness to the system for dealing with matched disturbance and mismatched parametric uncertainty. The bounds of uncertainty and disturbance are set in the Hamiltonian and cost function to provide a new control law that regulates the disturbed uncertain system.

The optimality of the conventional SDRE and the nonlinear design of the controller are great advantages though the sensitivity to uncertainty and disturbance could be listed as weak points. This work added a nonlinear mechanism in the weighting matrices of the system to include the bounds of disturbance and uncertainty to cover this problem. The unified design of the proposed robust SDRE is an important feature that implies simplicity in the design procedure. The complexity that the proposed design could handle is the capability to control the system with uncertainty and disturbance; additionally, it can handle disturbance with a shift in the steady-state value. This shift in the steady-state value moves the equilibrium of the system from zero to another point, which not all the controllers could observe and compensate that.

Section 2 presents the main results and tuning rules for providing stability and robust characteristics for the system. Section 3 presents the simulation results and Section 4 presents the comparison of the proposed controller with conventional robust designs and performs an analysis. Section 5 states the summary of the work.

Notations: $\mathbb{R}^n$ is the n-dimensional Euclidean space, $\mathbb{R}^{n\times m}$ is a set of

$n \times m$ real matrix; $(\cdot)^\top$ denotes a transposition of a matrix or a vector; $\mathbf{I}_{n\times n}$ and $\mathbf{0}_{n\times n}$ show $n \times n$ identity and zero matrices. $(\cdot)^\dagger$ performs a generalized inverse of a matrix and rand$(\cdot)$ generates a random number between $[0, 1]$.

2. Main Results

Consider a time-invariant nonlinear affine-in-control system with matched time-varying disturbance and mismatched parametric uncertainty:

$$\dot{\mathbf{x}}(t) = \mathbf{A}(\mathbf{x}(t), \boldsymbol{\eta})\mathbf{x}(t) + \mathbf{B}(\mathbf{x}(t), \boldsymbol{\eta})(\mathbf{u}(t) + \mathbf{w}(\mathbf{x}(t), t)), \tag{1}$$

where the state vector is presented by $\mathbf{x}(t) \in \mathbb{R}^n$, $\mathbf{u}(t) \in \mathbb{R}^m$ is an input vector, $\boldsymbol{\eta} \in \mathbb{R}^p$ is a vector of parameter uncertainty, where $\boldsymbol{\eta} \geq \mathbf{0}$, and it is limited to the upper bound $\boldsymbol{\eta} \leq \boldsymbol{\eta}_0$; $\mathbf{A}(\mathbf{x}(t), \boldsymbol{\eta}) : \mathbb{R}^n \times \mathbb{R}^p \to \mathbb{R}^{n\times n}$ and $\mathbf{B}(\mathbf{x}(t), \boldsymbol{\eta}) : \mathbb{R}^n \times \mathbb{R}^p \to \mathbb{R}^{n\times m}$ represent state-dependent coefficient parameterization of the dynamics

$$\dot{\mathbf{x}}(t) = \mathbf{f}(\mathbf{x}(t), \boldsymbol{\eta}) + \mathbf{g}(\mathbf{x}(t), \boldsymbol{\eta}, \mathbf{u}(t), t), \tag{2}$$

in which $\mathbf{f}(\mathbf{x}(t), \boldsymbol{\eta})$ and $\mathbf{g}(\mathbf{x}(t), \boldsymbol{\eta}, \mathbf{u}(t), t)$ are smooth piecewise-continuous vector-valued functions for all $\mathbf{x}(t) \in \mathbb{R}^n$ in $t \in \mathbb{R}^+$. The equilibrium point is zero $\mathbf{f}(\mathbf{0}, \boldsymbol{\eta}) = \mathbf{0}$, and $\mathbf{B}(\mathbf{0}, \boldsymbol{\eta}) \neq \mathbf{0}$. Moreover, $\mathbf{w}(\mathbf{x}(t), t) : \mathbb{R}^n \times \mathbb{R}^+ \to \mathbb{R}^m$ represents an unknown external disturbance vector.

Assumption 1. *The disturbance vector is bounded and smooth with a steady-state value,* $\mathbf{w}_\mathrm{b}$ *in* $t \in \mathbb{R}^+$ *where* $\lim_{t\to\infty} \mathbf{w}(\mathbf{x}(t), t) = \mathbf{w}_\mathrm{b}$. *Additionally,* $\mathbf{w}(\mathbf{x}(t), t) \leq \mathbf{w}_\mathrm{u}$ *holds in transient response and in steady-state condition* $\mathbf{w}_\mathrm{b} < \mathbf{w}_\mathrm{u}$.

Remark 1. *It should be noted that the system's equilibrium point without input is zero,* $\mathbf{f}(\mathbf{0}, \boldsymbol{\eta}) = \mathbf{0}$*; however, the matched disturbance has a steady-state shift,* $\mathbf{w}_\mathrm{b}$*, which imposes a non-zero equilibrium point for the whole system* $\dot{\mathbf{x}}(t)$*, depending on the disturbance.*

Assumption 2. *The pair of* $\{\mathbf{A}(\mathbf{x}(t), \boldsymbol{\eta}), \mathbf{B}(\mathbf{x}(t), \boldsymbol{\eta})\}$ *is a completely controllable parameterization of the system* (2) *for all* $\mathbf{x}(t)$ *in* $t \in \mathbb{R}^+$. $\boldsymbol{\eta}$ *makes* $\{\mathbf{A}(\mathbf{x}(t), \boldsymbol{\eta}), \mathbf{B}(\mathbf{x}(t), \boldsymbol{\eta})\}$ *uncertain though it does not affect the controllability.*

A brief example to clarify Assumption 2 is the pair of $\mathbf{A}(\mathbf{x}) = \begin{bmatrix} 0 & 1 \\ 0 & -x_2 \end{bmatrix}$ and $\mathbf{B}(\mathbf{x}) = \begin{bmatrix} 0 \\ 1 + x_1^2 \end{bmatrix}$ which is controllable, and adding parametric uncertainty changes the pair to $\mathbf{A}(\mathbf{x}, \boldsymbol{\eta}) = \begin{bmatrix} 0 & 1 + \eta_1 \\ 0 & -\eta_2 x_2 \end{bmatrix}$ and $\mathbf{B}(\mathbf{x}, \boldsymbol{\eta}) = \begin{bmatrix} 0 \\ 1 + \eta_1 x_1^2 \end{bmatrix}$, which make the system uncertain though the controllability matrix will not lose its rank, $\mathbf{M}_{\mathrm{c}}(\mathbf{x}, \boldsymbol{\eta}) = \begin{bmatrix} 0 & (1 + \eta_1)(1 + \eta_1 x_1^2) \\ 1 + \eta_1 x_1^2 & -\eta_2 x_2 (1 + \eta_1 x_1^2) \end{bmatrix}$ in the range of $0 \leq \boldsymbol{\eta} \leq \boldsymbol{\eta}_0$. Assumption 2 makes sure that the change in the uncertainty does not violate the controllability. The same will be held on Assumption 3 on observability condition.

The control aims to look for admissible input $\mathbf{u}(t)$ such that the state vector $\mathbf{x}(t)$, will be regulated to the equilibrium point of the system (1), $\mathbf{f}(\mathbf{0}, \boldsymbol{\eta}) = \mathbf{0}$, and the following cost function is minimized:

$$J(\cdot) = \frac{1}{2} \int_0^\infty \{(\mathbf{u}(t) + \mathbf{w}_{\mathrm{b}})^\top \mathbf{R}(\mathbf{x}(t))(\mathbf{u}(t) + \mathbf{w}_{\mathrm{b}}) + \mathbf{x}^\top(t) \mathbf{Q}(\mathbf{x}(t)) \mathbf{x}(t)\} \, \mathrm{d}t, \quad (3)$$

where $\mathbf{Q}(\mathbf{x}(t)) : \mathbb{R}^n \to \mathbb{R}^{n \times n}$ and $\mathbf{R}(\mathbf{x}(t)) : \mathbb{R}^n \to \mathbb{R}^{m \times m}$ are positive-semidefinite and positive-definite symmetric matrices, respectively.

Assumption 3. *The pair of* $\{\mathbf{A}(\mathbf{x}(t), \boldsymbol{\eta}), \mathbf{Q}^{1/2}(\mathbf{x}(t))\}$ *is a completely observable parameterization of the system* (2) *and weighting matrix of states in cost function* (3) *for all* $\mathbf{x}(t)$ *in* $t \in \mathbb{R}^+$*, where* $\mathbf{Q}^{1/2}(\mathbf{x}(t))$ *is the Cholesky decomposition of* $\mathbf{Q}^{1/2}(\mathbf{x}(t))$*. Similar to Assumption 2,* $\boldsymbol{\eta}$ *does not violate the observability condition.*

The controllability and observability conditions, presented in Assumptions 2 and 3, are checked through the computation of the rank of the controllability matrix:

$$\mathcal{M}_{\mathrm{c}} = \begin{bmatrix} \mathbf{B}(\mathbf{x}(t), \boldsymbol{\eta}) & \mathbf{A}(\mathbf{x}(t), \boldsymbol{\eta}) \mathbf{B}(\mathbf{x}(t), \boldsymbol{\eta}) & \cdots & \mathbf{A}^{n-1}(\mathbf{x}(t), \boldsymbol{\eta}) \mathbf{B}(\mathbf{x}(t), \boldsymbol{\eta}) \end{bmatrix},$$

and observability matrix:

$$\mathcal{M}_{\mathrm{o}} = \begin{bmatrix} \mathbf{Q}^{1/2}(\mathbf{x}(t)) \\ \mathbf{Q}^{1/2}(\mathbf{x}(t)) \mathbf{A}(\mathbf{x}(t), \boldsymbol{\eta}) \\ \vdots \\ \mathbf{Q}^{1/2}(\mathbf{x}(t)) \mathbf{A}^{n-1}(\mathbf{x}(t), \boldsymbol{\eta}) \end{bmatrix}.$$

If matrices $\mathcal{M}_{\rm c}$ and $\mathcal{M}_{\rm o}$ are fully ranked, equal to n, in the time interval $t \in [0, t_{\rm f}]$, then Assumptions 2 and 3 are satisfied.

To derive the Riccati equation and the control law, the information on the bounds will be considered in the design since the real matrices are unknown. If the unknown system is denoted by $\mathbf{A}(\mathbf{x}(t), \boldsymbol{\eta}), \mathbf{B}(\mathbf{x}(t), \boldsymbol{\eta}), \mathbf{w}(\mathbf{x}(t), t)$, considering the known bounds, one could define $\mathbf{A}(\mathbf{x}(t), \boldsymbol{\eta}_0), \mathbf{B}(\mathbf{x}(t), \boldsymbol{\eta}_0), \mathbf{w}_{\rm b}$ to design the control law and corresponding Riccati equation. The upper bound of uncertainty could be set by the designer, based on the physical characteristics of the model, i.e. the maximum mass/load of one component ($\eta_1 = m_1(\text{kg}), f_1(\text{N})$ is the unknown parameter and $\eta_{0,1} = m_{1,\max}(\text{kg}), f_{1,\max}(\text{N})$ is the maximum value) such as a link of a robotic manipulator or the friction force of that link ($\eta_2 = f_{\text{fr},1}(\text{N})$ is the unknown and $\eta_{0,2} = f_{\text{fr},1,\max}(\text{N})$ is the maximum value). The upper bound of uncertain values results in corresponding dynamics and SDC matrices, $\mathbf{A}(\mathbf{x}(t), \boldsymbol{\eta}_0), \mathbf{B}(\mathbf{x}(t), \boldsymbol{\eta}_0)$.

Shaping the Hamiltonian with the information of the known system considering η_0 and $\mathbf{w}_{\rm b}$, provides:

$$\begin{aligned}\mathcal{H}(\mathbf{x}(t), \boldsymbol{\eta}, \mathbf{u}(t), \boldsymbol{\lambda}(t), t) = \frac{1}{2}\{(\mathbf{u}(t) + \mathbf{w}_{\rm b})^\top \mathbf{R}(\mathbf{x}(t))(\mathbf{u}(t) + \mathbf{w}_{\rm b}) + \\ \mathbf{x}^\top(t)\mathbf{Q}(\mathbf{x}(t))\mathbf{x}(t)\} + \boldsymbol{\lambda}^\top(t)[\mathbf{A}(\mathbf{x}(t), \boldsymbol{\eta}_0)\mathbf{x}(t) + \mathbf{B}(\mathbf{x}(t), \boldsymbol{\eta}_0)(\mathbf{u}(t) + \mathbf{w}_{\rm b})],\end{aligned}$$

where $\boldsymbol{\lambda}(t) = \mathbf{K}(\mathbf{x}(t), \boldsymbol{\eta}_0)\mathbf{x}(t)$ is a co-state vector and it follows:

$$\dot{\boldsymbol{\lambda}}(t) = \mathbf{K}(\mathbf{x}(t), \boldsymbol{\eta}_0)\dot{\mathbf{x}}(t) + \dot{\mathbf{K}}(\mathbf{x}(t), \boldsymbol{\eta}_0)\mathbf{x}(t).$$

Now, by considering the optimality conditions [3]:

$$\begin{aligned}\frac{\partial \mathcal{H}(\cdot)}{\partial \mathbf{x}(t)} &= -\dot{\boldsymbol{\lambda}}(t), \\ \frac{\partial \mathcal{H}(\cdot)}{\partial \boldsymbol{\lambda}(t)} &= \dot{\mathbf{x}}(t), \\ \frac{\partial \mathcal{H}(\cdot)}{\partial \mathbf{u}(t)} &= \mathbf{0},\end{aligned} \tag{4}$$

the control law and the robust SDRE equation will be obtained. Considering the third condition in (4), one could find

$$\mathbf{B}^\top(\mathbf{x}(t), \boldsymbol{\eta}_0)\boldsymbol{\lambda}(t) + \mathbf{R}(\mathbf{x}(t))(\mathbf{u}(t) + \mathbf{w}_{\rm b}) = \mathbf{0},$$

and with the co-state vector definition, then the control law is found:

$$\mathbf{u}(t) = -\mathbf{R}^{-1}(\mathbf{x}(t))\mathbf{B}^{\top}(\mathbf{x}(t), \boldsymbol{\eta}_0)\mathbf{K}(\mathbf{x}(t), \boldsymbol{\eta}_0)\mathbf{x}(t) - \mathbf{w}_{\mathrm{b}}, \tag{5}$$

in which $\mathbf{K}(\mathbf{x}(t), \boldsymbol{\eta}_0) : \mathbb{R}^n \times \mathbb{R}^p \to \mathbb{R}^{n \times n}$ is the symmetric positive definite sub-optimal gain of the controller. The second condition of (4) satisfies system equation (1), by substituting $\boldsymbol{\eta} \to \boldsymbol{\eta}_0$ and $\mathbf{w}(\mathbf{x}(t), t) \to \mathbf{w}_{\mathrm{b}}$. To find the Riccati equation, the first condition is used which results in:

$$\begin{aligned}
\frac{\partial \mathcal{H}(\cdot)}{\partial \mathbf{x}(t)} =& \mathbf{Q}(\mathbf{x}(t))\mathbf{x}(t) + \frac{1}{2}\mathbf{x}^{\top}(t)\left(\frac{\partial \mathbf{Q}(\mathbf{x}(t))}{\partial \mathbf{x}(t)}\right)^{\top}\mathbf{x}(t) + \mathbf{A}^{\top}(\mathbf{x}(t), \boldsymbol{\eta}_0)\boldsymbol{\lambda}(t) \\
&+ \mathbf{x}^{\top}(t)\left(\frac{\partial \mathbf{A}(\mathbf{x}(t), \boldsymbol{\eta}_0)}{\partial \mathbf{x}(t)}\right)^{\top}\boldsymbol{\lambda}(t) + \frac{1}{2}(\mathbf{u}(t) + \mathbf{w}_{\mathrm{b}})^{\top}\left(\frac{\partial \mathbf{R}(\mathbf{x}(t))}{\partial \mathbf{x}(t)}\right)^{\top} \\
&(\mathbf{u}(t) + \mathbf{w}_{\mathrm{b}}) + (\mathbf{u}(t) + \mathbf{w}_{\mathrm{b}})^{\top}\left(\frac{\partial \mathbf{B}(\mathbf{x}(t), \boldsymbol{\eta}_0)}{\partial \mathbf{x}(t)}\right)^{\top}\boldsymbol{\lambda}(t) = \\
&- \dot{\mathbf{K}}(\mathbf{x}(t), \boldsymbol{\eta}_0)\mathbf{x}(t) - \mathbf{K}(\mathbf{x}(t), \boldsymbol{\eta}_0)\dot{\mathbf{x}}(t).
\end{aligned} \tag{6}$$

Substituting system (1) with its known bounds and steady-state value of disturbance $\mathbf{w}_{\mathrm{b}}$, co-state vector and control law (5) into (6), one could present (t argument is removed for simplification):

$$\begin{aligned}
&\mathbf{Q}(\mathbf{x})\mathbf{x} + \frac{1}{2}\mathbf{x}^{\top}\left(\frac{\partial \mathbf{Q}(\mathbf{x})}{\partial \mathbf{x}}\right)^{\top}\mathbf{x} + \frac{1}{2}\mathbf{x}^{\top}\mathbf{K}(\mathbf{x}, \boldsymbol{\eta}_0)\mathbf{B}(\mathbf{x}, \boldsymbol{\eta}_0)\mathbf{R}^{-1}(\mathbf{x})\left(\frac{\partial \mathbf{R}(\mathbf{x})}{\partial \mathbf{x}}\right)^{\top} \\
&\mathbf{R}^{-1}(\mathbf{x})\mathbf{B}^{\top}(\mathbf{x}, \boldsymbol{\eta}_0)\mathbf{K}(\mathbf{x}, \boldsymbol{\eta}_0)\mathbf{x} - \mathbf{x}^{\top}\mathbf{K}(\mathbf{x}, \boldsymbol{\eta}_0)\mathbf{B}(\mathbf{x}, \boldsymbol{\eta}_0)\mathbf{R}^{-1}(\mathbf{x}) \\
&\left(\frac{\partial \mathbf{B}(\mathbf{x}, \boldsymbol{\eta}_0)}{\partial \mathbf{x}}\right)^{\top}\mathbf{K}(\mathbf{x}, \boldsymbol{\eta}_0)\mathbf{x} + \mathbf{A}^{\top}(\mathbf{x}, \boldsymbol{\eta}_0)\mathbf{K}(\mathbf{x}, \boldsymbol{\eta}_0)\mathbf{x} + \\
&\mathbf{x}^{\top}\left(\frac{\partial \mathbf{A}(\mathbf{x}, \boldsymbol{\eta}_0)}{\partial \mathbf{x}}\right)^{\top}\mathbf{K}(\mathbf{x}, \boldsymbol{\eta}_0)\mathbf{x} = \\
&\mathbf{K}(\mathbf{x}, \boldsymbol{\eta}_0)\mathbf{B}(\mathbf{x}, \boldsymbol{\eta}_0)\mathbf{R}^{-1}(\mathbf{x})\mathbf{B}^{\top}(\mathbf{x}, \boldsymbol{\eta}_0)\mathbf{K}(\mathbf{x}, \boldsymbol{\eta}_0)\mathbf{x} \\
&- \dot{\mathbf{K}}(\mathbf{x}, \boldsymbol{\eta}_0)\mathbf{x} - \mathbf{K}(\mathbf{x}, \boldsymbol{\eta}_0)\mathbf{A}(\mathbf{x}, \boldsymbol{\eta}_0)\mathbf{x}.
\end{aligned} \tag{7}$$

Equation (7) is simplified as:

$$
\begin{aligned}
&\{-\mathbf{K}(\mathbf{x},\boldsymbol{\eta}_0)\mathbf{B}(\mathbf{x},\boldsymbol{\eta}_0)\mathbf{R}^{-1}(\mathbf{x})\mathbf{B}^\top(\mathbf{x},\boldsymbol{\eta}_0)\mathbf{K}(\mathbf{x},\boldsymbol{\eta}_0)+\mathbf{K}(\mathbf{x},\boldsymbol{\eta}_0)\\
&\quad\mathbf{A}(\mathbf{x},\boldsymbol{\eta}_0)+\mathbf{A}^\top(\mathbf{x},\boldsymbol{\eta}_0)\mathbf{K}(\mathbf{x},\boldsymbol{\eta}_0)+\mathbf{Q}(\mathbf{x})\}\mathbf{x}+\\
&\quad\Bigg[\dot{\mathbf{K}}(\mathbf{x},\boldsymbol{\eta}_0)+\frac{1}{2}\mathbf{x}^\top\left(\frac{\partial\mathbf{Q}(\mathbf{x})}{\partial\mathbf{x}}\right)^\top+\frac{1}{2}\mathbf{x}^\top\mathbf{K}(\mathbf{x},\boldsymbol{\eta}_0)\mathbf{B}(\mathbf{x},\boldsymbol{\eta}_0)\\
&\quad\mathbf{R}^{-1}(\mathbf{x})\left(\frac{\partial\mathbf{R}(\mathbf{x})}{\partial\mathbf{x}}\right)^\top\mathbf{R}^{-1}(\mathbf{x})\mathbf{B}^\top(\mathbf{x},\boldsymbol{\eta}_0)\mathbf{K}(\mathbf{x},\boldsymbol{\eta}_0)+\\
&\quad\mathbf{x}^\top\left(\frac{\partial\mathbf{A}(\mathbf{x},\boldsymbol{\eta}_0)}{\partial\mathbf{x}}\right)^\top\mathbf{K}(\mathbf{x},\boldsymbol{\eta}_0)-\mathbf{x}^\top\mathbf{K}(\mathbf{x},\boldsymbol{\eta}_0)\mathbf{B}(\mathbf{x},\boldsymbol{\eta}_0)\mathbf{R}^{-1}(\mathbf{x})\\
&\quad\left(\frac{\partial\mathbf{B}(\mathbf{x},\boldsymbol{\eta}_0)}{\partial\mathbf{x}}\right)^\top\mathbf{K}(\mathbf{x},\boldsymbol{\eta}_0)\Bigg]\mathbf{x}=\mathbf{0}.
\end{aligned}
\tag{8}
$$

Equation (8) has two parts, the robust SDRE:

$$
\begin{aligned}
&\mathbf{K}(\mathbf{x},\boldsymbol{\eta}_0)\mathbf{A}(\mathbf{x},\boldsymbol{\eta}_0)+\mathbf{A}^\top(\mathbf{x},\boldsymbol{\eta}_0)\mathbf{K}(\mathbf{x},\boldsymbol{\eta}_0)+\\
&\qquad\mathbf{Q}(\mathbf{x})-\mathbf{K}(\mathbf{x},\boldsymbol{\eta}_0)\mathbf{B}(\mathbf{x},\boldsymbol{\eta}_0)\mathbf{R}^{-1}(\mathbf{x})\mathbf{B}^\top(\mathbf{x},\boldsymbol{\eta}_0)\mathbf{K}(\mathbf{x},\boldsymbol{\eta}_0)=\mathbf{0},
\end{aligned}
\tag{9}
$$

and the necessary condition for optimality:

$$
\begin{aligned}
&\dot{\mathbf{K}}(\mathbf{x},\boldsymbol{\eta}_0)+\frac{1}{2}\left(\frac{\partial\mathbf{Q}(\mathbf{x})}{\partial\mathbf{x}}\mathbf{x}\right)^\top+\frac{1}{2}\left(\frac{\partial\mathbf{R}(\mathbf{x})}{\partial\mathbf{x}}[\mathbf{R}^{-1}(\mathbf{x})\mathbf{B}^\top(\mathbf{x},\boldsymbol{\eta}_0)\mathbf{K}(\mathbf{x},\boldsymbol{\eta}_0)\mathbf{x}]\right)^\top\\
&\quad\mathbf{R}^{-1}(\mathbf{x})\mathbf{B}^\top(\mathbf{x},\boldsymbol{\eta}_0)\mathbf{K}(\mathbf{x},\boldsymbol{\eta}_0)+\left(\frac{\partial\mathbf{A}(\mathbf{x},\boldsymbol{\eta}_0)}{\partial\mathbf{x}}\mathbf{x}\right)^\top\mathbf{K}(\mathbf{x},\boldsymbol{\eta}_0)-\\
&\quad\left(\frac{\partial\mathbf{B}(\mathbf{x},\boldsymbol{\eta}_0)}{\partial\mathbf{x}}[\mathbf{R}^{-1}(\mathbf{x})\mathbf{B}^\top(\mathbf{x},\boldsymbol{\eta}_0)\mathbf{K}(\mathbf{x},\boldsymbol{\eta}_0)\mathbf{x}]\right)^\top\mathbf{K}(\mathbf{x},\boldsymbol{\eta}_0)=\mathbf{0}.
\end{aligned}
$$

Theorem 1. *Considering Assumptions 1-3, the nonlinear system* (1) *with parameter uncertainty and matched disturbance, is stabilized using control law* (5)*, where the control gain* $\mathbf{K}(\mathbf{x}(t),\boldsymbol{\eta}_0)$ *is the symmetric positive-definite solution to the robust SDRE* (9)*, if the weighting matrices,* $\mathbf{R}(\mathbf{x}(t))$ *and* $\mathbf{Q}(\mathbf{x}(t))$ *are defined as:*

$$
\epsilon\mathbf{I}_{m\times m}\leq\mathbf{R}(\mathbf{x}(t))<\left(\mathbf{B}^\dagger(\mathbf{x}(t),\boldsymbol{\eta}_0)[\mathbf{B}^\top(\mathbf{x}(t),\boldsymbol{\eta}_0)]^\dagger\right)^{-1},
\tag{10}
$$

$$
\mathbf{Q}_{\mathrm{b}}(\mathbf{x}(t))<\mathbf{Q}(\mathbf{x}(t))\leq\mathbf{Q}_{\max},
\tag{11}
$$

in which $0 < \epsilon \ll 1$, *and*

$$\mathbf{Q}_{\mathrm{b}}(\mathbf{x}(t)) = [\mathbf{x}^{\dagger}(t)]^{\top}[\mathbf{w}_{\mathrm{u}} - \mathbf{w}_{\mathrm{b}}]^{\top}\mathbf{B}^{\top}(\mathbf{x}(t), \boldsymbol{\eta}_0)\mathbf{B}(\mathbf{x}(t), \boldsymbol{\eta}_0)[\mathbf{w}_{\mathrm{u}} - \mathbf{w}_{\mathrm{b}}]\mathbf{x}^{\dagger}(t), \quad (12)$$

moreover, the upper bound is symmetric positive-definite $\mathbf{Q}_{\max} \gg \mathbf{I}_{n\times n}$.

Proof: To check the stability of the system, a Lyapunov candidate is chosen as $V(\mathbf{x}(t), \boldsymbol{\eta}_0) = \mathbf{x}^{\top}(t)\mathbf{K}(\mathbf{x}(t), \boldsymbol{\eta}_0)\mathbf{x}(t)$, which is $V(\mathbf{x}(t), \boldsymbol{\eta}_0) > 0$ when $\mathbf{x}(t) \neq \mathbf{0}$; $V(\mathbf{x}(t), \boldsymbol{\eta}_0) = 0$ when $\mathbf{x}(t) = \mathbf{0}$. The derivative of the Lyapunov function results in

$$\begin{aligned}\dot{V}(\mathbf{x}(t), \boldsymbol{\eta}_0) =& \dot{\mathbf{x}}^{\top}(t)\mathbf{K}(\mathbf{x}(t), \boldsymbol{\eta}_0)\mathbf{x}(t) + \mathbf{x}^{\top}(t)\dot{\mathbf{K}}(\mathbf{x}(t), \boldsymbol{\eta}_0)\mathbf{x}(t) + \\ & \mathbf{x}^{\top}(t)\mathbf{K}(\mathbf{x}(t), \boldsymbol{\eta}_0)\dot{\mathbf{x}}(t).\end{aligned} \quad (13)$$

To guarantee the stability of the uncertain system, Eq. (1) is substituted into (13). The algebraic form of the robust SDRE was also considered for solving the optimal control, $t \to \infty$ based on cost function (3) then $\lim_{t\to\infty} \mathbf{K}(\mathbf{x}(t), \boldsymbol{\eta}_0) = \mathbf{K}_{\mathrm{ss}}(\mathbf{x}(\infty), \boldsymbol{\eta}_0)$, and $\dot{\mathbf{K}}(\mathbf{x}(t), \boldsymbol{\eta}_0) = \mathbf{0}$ is removed from (13) which results in

$$\begin{aligned}\dot{V}(\mathbf{x}, \boldsymbol{\eta}_0) =& \mathbf{x}^{\top}\mathbf{A}^{\top}(\mathbf{x}, \boldsymbol{\eta})\mathbf{K}(\mathbf{x}, \boldsymbol{\eta}_0)\mathbf{x} + \mathbf{u}^{\top}\mathbf{B}^{\top}(\mathbf{x}, \boldsymbol{\eta})\mathbf{K}(\mathbf{x}, \boldsymbol{\eta}_0)\mathbf{x} + \\ & \mathbf{w}^{\top}(\mathbf{x}, t)\mathbf{B}^{\top}(\mathbf{x}, \boldsymbol{\eta})\mathbf{K}(\mathbf{x}, \boldsymbol{\eta}_0)\mathbf{x} + \mathbf{x}^{\top}\mathbf{K}(\mathbf{x}, \boldsymbol{\eta}_0)\mathbf{A}(\mathbf{x}, \boldsymbol{\eta})\mathbf{x} + \\ & \mathbf{x}^{\top}\mathbf{K}(\mathbf{x}, \boldsymbol{\eta}_0)\mathbf{B}(\mathbf{x}, \boldsymbol{\eta})\mathbf{u} + \mathbf{x}^{\top}\mathbf{K}(\mathbf{x}, \boldsymbol{\eta}_0)\mathbf{B}(\mathbf{x}, \boldsymbol{\eta})\mathbf{w}(\mathbf{x}, t).\end{aligned} \quad (14)$$

Substituting control law (5) into (14) also generates

$$\begin{aligned}\dot{V}(\mathbf{x}, \boldsymbol{\eta}_0) =& \mathbf{x}^{\top}\mathbf{A}^{\top}(\mathbf{x}, \boldsymbol{\eta})\mathbf{K}(\mathbf{x}, \boldsymbol{\eta}_0)\mathbf{x} - \mathbf{x}^{\top}\mathbf{K}(\mathbf{x}, \boldsymbol{\eta}_0)\mathbf{B}(\mathbf{x}, \boldsymbol{\eta}_0)\mathbf{R}^{-1}(\mathbf{x}) \\ & \mathbf{B}^{\top}(\mathbf{x}, \boldsymbol{\eta})\mathbf{K}(\mathbf{x}, \boldsymbol{\eta}_0)\mathbf{x} - \mathbf{w}_{\mathrm{b}}^{\top}\mathbf{B}^{\top}(\mathbf{x}, \boldsymbol{\eta})\mathbf{K}(\mathbf{x}, \boldsymbol{\eta}_0)\mathbf{x} + \\ & \mathbf{w}^{\top}(\mathbf{x}, t)\mathbf{B}^{\top}(\mathbf{x}, \boldsymbol{\eta})\mathbf{K}(\mathbf{x}, \boldsymbol{\eta}_0)\mathbf{x} + \mathbf{x}^{\top}\mathbf{K}(\mathbf{x}, \boldsymbol{\eta}_0)\mathbf{A}(\mathbf{x}, \boldsymbol{\eta})\mathbf{x} - \\ & \mathbf{x}^{\top}\mathbf{K}(\mathbf{x}, \boldsymbol{\eta}_0)\mathbf{B}(\mathbf{x}, \boldsymbol{\eta})\mathbf{R}^{-1}(\mathbf{x})\mathbf{B}^{\top}(\mathbf{x}, \boldsymbol{\eta}_0)\mathbf{K}(\mathbf{x}, \boldsymbol{\eta}_0)\mathbf{x} - \\ & \mathbf{x}^{\top}\mathbf{K}(\mathbf{x}, \boldsymbol{\eta}_0)\mathbf{B}(\mathbf{x}, \boldsymbol{\eta})\mathbf{w}_{\mathrm{b}} + \mathbf{x}^{\top}\mathbf{K}(\mathbf{x}, \boldsymbol{\eta}_0)\mathbf{B}(\mathbf{x}, \boldsymbol{\eta})\mathbf{w}(\mathbf{x}, t).\end{aligned} \quad (15)$$

Considering the known bounds of $\mathbf{A}(\mathbf{x}, \boldsymbol{\eta}_0)$ and $\mathbf{B}(\mathbf{x}, \boldsymbol{\eta}_0)$ for (15), and substituting

$$\begin{aligned}&\mathbf{K}(\mathbf{x}, \boldsymbol{\eta}_0)\mathbf{A}(\mathbf{x}, \boldsymbol{\eta}_0) + \mathbf{A}^{\top}(\mathbf{x}, \boldsymbol{\eta}_0)\mathbf{K}(\mathbf{x}, \boldsymbol{\eta}_0) - \\ &\quad \mathbf{K}(\mathbf{x}, \boldsymbol{\eta}_0)\mathbf{B}(\mathbf{x}, \boldsymbol{\eta}_0)\mathbf{R}^{-1}(\mathbf{x})\mathbf{B}^{\top}(\mathbf{x}, \boldsymbol{\eta}_0)\mathbf{K}(\mathbf{x}, \boldsymbol{\eta}_0) = -\mathbf{Q}(\mathbf{x}),\end{aligned}$$

in the updated form of (15) result in

$$\begin{aligned}\dot{V}(\mathbf{x},\boldsymbol{\eta}_0) = &-\mathbf{x}^\top\mathbf{Q}(\mathbf{x})\mathbf{x}+\boldsymbol{\omega}^\top(\mathbf{x},\boldsymbol{\eta}_0,t)\mathbf{K}(\mathbf{x},\boldsymbol{\eta}_0)\mathbf{x}-\mathbf{x}^\top\mathbf{K}(\mathbf{x},\boldsymbol{\eta}_0)\mathbf{B}(\mathbf{x},\boldsymbol{\eta}_0)\\ &\mathbf{R}^{-1}(\mathbf{x})\mathbf{B}^\top(\mathbf{x},\boldsymbol{\eta}_0)\mathbf{K}(\mathbf{x},\boldsymbol{\eta}_0)\mathbf{x}+\mathbf{x}^\top\mathbf{K}(\mathbf{x},\boldsymbol{\eta}_0)\boldsymbol{\omega}(\mathbf{x},\boldsymbol{\eta}_0,t),\end{aligned} \tag{16}$$

where $\boldsymbol{\omega}(\mathbf{x},\boldsymbol{\eta}_0,t) = \mathbf{B}(\mathbf{x},\boldsymbol{\eta}_0)[-\mathbf{w}_\mathrm{b}+\mathbf{w}(\mathbf{x},t)]$. Since $\mathbf{K}(\mathbf{x},\boldsymbol{\eta}_0)$ is symmetric, Eq. (16) is simplified as

$$\begin{aligned}\dot{V}(\mathbf{x},\boldsymbol{\eta}_0) = &-\mathbf{x}^\top\mathbf{Q}(\mathbf{x})\mathbf{x}-\mathbf{x}^\top\mathbf{K}(\mathbf{x},\boldsymbol{\eta}_0)\mathbf{B}(\mathbf{x},\boldsymbol{\eta}_0)\mathbf{R}^{-1}(\mathbf{x})\\ &\mathbf{B}^\top(\mathbf{x},\boldsymbol{\eta}_0)\mathbf{K}(\mathbf{x},\boldsymbol{\eta}_0)\mathbf{x}+2\mathbf{x}^\top\mathbf{K}(\mathbf{x},\boldsymbol{\eta}_0)\boldsymbol{\omega}(\mathbf{x},\boldsymbol{\eta}_0,t),\end{aligned} \tag{17}$$

and it must be less than zero to guarantee stability. Recalling Young's inequality for products, one could rewrite (17) as:

$$\begin{aligned}\dot{V}(\mathbf{x},\boldsymbol{\eta}_0) = &-\mathbf{x}^\top\mathbf{Q}(\mathbf{x})\mathbf{x}-\mathbf{x}^\top\mathbf{K}(\mathbf{x},\boldsymbol{\eta}_0)\mathbf{B}(\mathbf{x},\boldsymbol{\eta}_0)\mathbf{R}^{-1}(\mathbf{x})\mathbf{B}^\top(\mathbf{x},\boldsymbol{\eta}_0)\mathbf{K}(\mathbf{x},\boldsymbol{\eta}_0)\mathbf{x}+\\ &\mathbf{x}^\top\mathbf{K}(\mathbf{x},\boldsymbol{\eta}_0)\mathbf{K}(\mathbf{x},\boldsymbol{\eta}_0)\mathbf{x}+\boldsymbol{\omega}^\top(\mathbf{x},\boldsymbol{\eta}_0,t)\boldsymbol{\omega}(\mathbf{x},\boldsymbol{\eta}_0,t)<0,\end{aligned} \tag{18}$$

where $\mathbf{K}^\top(\mathbf{x},\boldsymbol{\eta}_0) = \mathbf{K}(\mathbf{x},\boldsymbol{\eta}_0)$. Equation (18) is rearranged as

$$\begin{aligned}\dot{V}(\mathbf{x},\boldsymbol{\eta}_0) = &-\mathbf{x}^\top\{\mathbf{Q}(\mathbf{x})-[\mathbf{x}^\dagger]^\top\boldsymbol{\omega}^\top(\mathbf{x},\boldsymbol{\eta}_0,t)\boldsymbol{\omega}(\mathbf{x},\boldsymbol{\eta}_0,t)\mathbf{x}^\dagger\}\mathbf{x}-\\ &\mathbf{x}^\top[\mathbf{K}(\mathbf{x},\boldsymbol{\eta}_0)\mathbf{B}(\mathbf{x},\boldsymbol{\eta}_0)\mathbf{R}^{-1}(\mathbf{x})\mathbf{B}^\top(\mathbf{x},\boldsymbol{\eta}_0)\\ &\mathbf{K}(\mathbf{x},\boldsymbol{\eta}_0)-\mathbf{K}(\mathbf{x},\boldsymbol{\eta}_0)\mathbf{K}(\mathbf{x},\boldsymbol{\eta}_0)]\mathbf{x}<0,\end{aligned}$$

which forces the system to follow two tuning rules for weighting matrices:

$$\mathbf{Q}(\mathbf{x}(t)) > [\mathbf{x}^\dagger(t)]^\top\boldsymbol{\omega}^\top(\mathbf{x}(t),\boldsymbol{\eta}_0,t)\boldsymbol{\omega}(\mathbf{x}(t),\boldsymbol{\eta}_0,t)\mathbf{x}^\dagger(t), \tag{19}$$

$$\mathbf{B}(\mathbf{x}(t),\boldsymbol{\eta}_0)\mathbf{R}^{-1}(\mathbf{x}(t))\mathbf{B}^\top(\mathbf{x}(t),\boldsymbol{\eta}_0) > \mathbf{I}_{n\times n}. \tag{20}$$

Based on Assumption 1, the upper bound of uncertainty, $\mathbf{w}_\mathrm{u}$, is substituted into (19) and (20) and they are rewritten as:

$$\mathbf{Q}_\mathrm{b}(\mathbf{x}(t)) < \mathbf{Q}(\mathbf{x}(t)), \tag{21}$$

$$\mathbf{R}(\mathbf{x}(t)) < \left(\mathbf{B}^\dagger(\mathbf{x}(t),\boldsymbol{\eta}_0)[\mathbf{B}^\top(\mathbf{x}(t),\boldsymbol{\eta}_0)]^\dagger\right)^{-1}, \tag{22}$$

where

$$\mathbf{Q}_\mathrm{b}(\mathbf{x}(t)) = [\mathbf{x}^\dagger(t)]^\top[\mathbf{w}_\mathrm{u}-\mathbf{w}_\mathrm{b}]^\top\mathbf{B}^\top(\mathbf{x}(t),\boldsymbol{\eta}_0)\mathbf{B}(\mathbf{x}(t),\boldsymbol{\eta}_0)[\mathbf{w}_\mathrm{u}-\mathbf{w}_\mathrm{b}]\mathbf{x}^\dagger(t).$$

Note that the unknown value $\mathbf{w}(\mathbf{x}(t),t)$ is replaced with its upper bound $\mathbf{w}_{\mathrm{u}}$ and therefore, $\mathbf{w}_{\mathrm{u}}-\mathbf{w}_{\mathrm{b}}>\mathbf{0}$, in (21). When the error goes to zero, $\mathbf{Q}_{\mathrm{b}}(\mathbf{x}(t))$ will gain a very large value, that will cause excessive use of control and chattering in the input signal. To avoid that problem, Eq. (21) is bounded above by:

$$\mathbf{Q}(\mathbf{x}(t))\leq\mathbf{Q}_{\max}, \tag{23}$$

where $\mathbf{Q}_{\max}\gg\mathbf{I}_{n\times n}$ and $\mathbf{Q}_{\max}^{\top}=\mathbf{Q}_{\max}$.

It was stated that $\mathbf{B}(\mathbf{x}(t),\boldsymbol{\eta}_0)\neq\mathbf{0}$, however, rarely it might gain a very small value. To make sure the definition of $\mathbf{R}(\mathbf{x}(t))$ is complete, a minimum value of ϵ is considered to limit the lower bound of $\epsilon\mathbf{I}_{m\times m}\leq\mathbf{R}(\mathbf{x}(t))$ where $0<\epsilon\ll 1$. Then the weighting matrices (21) and (22) are defined as:

$$\mathbf{Q}_{\mathrm{b}}(\mathbf{x}(t))<\mathbf{Q}(\mathbf{x}(t))\leq\mathbf{Q}_{\max},$$

$$\epsilon\mathbf{I}_{m\times m}\leq\mathbf{R}(\mathbf{x}(t))<\left(\mathbf{B}^{\dagger}(\mathbf{x}(t),\boldsymbol{\eta}_0)[\mathbf{B}^{\top}(\mathbf{x}(t),\boldsymbol{\eta}_0)]^{\dagger}\right)^{-1},$$

which concludes the proof. □

Remark 2. *Realization of Eq.* (23) *in implementation will be done by adding conditions on the value of components of* $\mathbf{Q}(\mathbf{x}(t))$*. If one of the diagonal components of* $\mathbf{Q}(\mathbf{x}(t))$ *reaches the bound* $\mathbf{Q}_{\max}$*, the condition will use* $\mathbf{Q}_{\max}$ *instead of* $\mathbf{Q}_{\mathrm{b}}(\mathbf{x}(t))$*. This does not violate the steady-state behavior of the tuning and the controller since when* $\mathbf{Q}_{\max}$ *is active, that means the Pseudo inverse of error,* $\mathbf{x}^{\dagger}(t)$*, possesses a very large value and consequently, the error possesses a very small value (a desirable result).*

To clarify the workflow of the proposed robust SDRE controller, the block diagram of the system is presented in Fig. 1.

3. Simulations

Consider an illustrative example, a fourth-order differential equation in state-space form, within the framework of system (1) with state-vector $\mathbf{x}(t)=[x_1(t),x_2(t),x_3(t),x_4(t)]^{\top}$ and a single input $u(t)$ that correspond to SDC matrices:

$$\mathbf{A}(\mathbf{x},\boldsymbol{\eta})=\begin{bmatrix}0 & 1+\eta_3 & 0 & 0\\ 0 & 0 & 1 & 0\\ 0 & 0 & 0 & 1+\eta_4\\ -\eta_4(x_1^2+x_2^2)e^{-|x_1|} & -4\eta_1\sin(x_1+x_3) & -0.6-\frac{1}{1+x_3^2+x_4^2}e^{-t} & -x_1\mathrm{sign}(x_1)+\eta_2+\cos(x_4)\end{bmatrix},$$

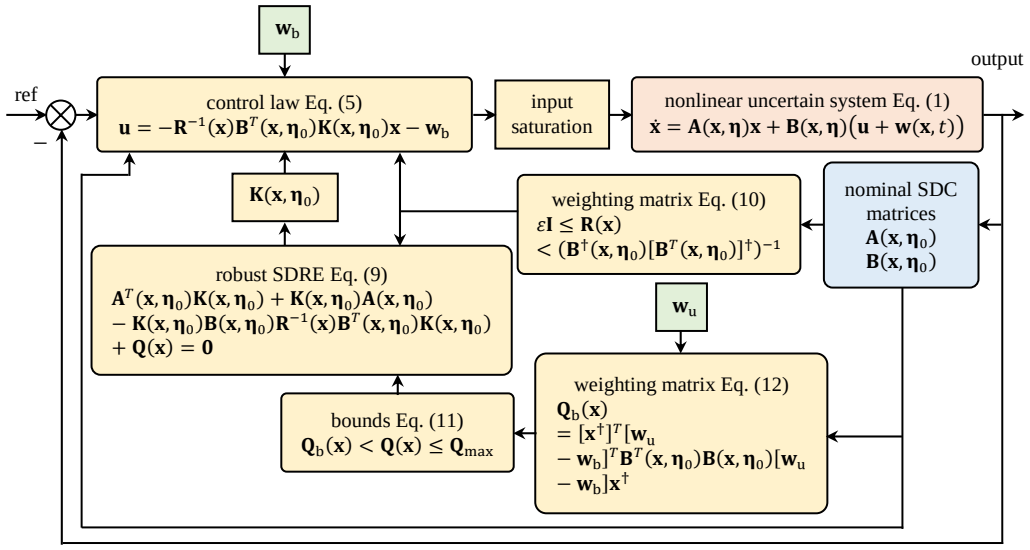

Figure 1: The block diagram of the robust SDRE controller design.

$$\mathbf{B} = [0, 0, 0, 1]^\top$$

where the unknown parameters are $\boldsymbol{\eta} = \mathrm{diag}(\mathrm{rand}(4,1))\boldsymbol{\eta}_0$, in which the upper bound is $\boldsymbol{\eta}_0 = [0.3, 0.4, 0.2, 0.15]^\top$ and $\mathrm{rand}(4,1)$ generates a random vector with four components between $[0,1]$ and diag makes it a diagonal matrix.

Remark 3. *The upper bound of $\boldsymbol{\eta}_0$ has been selected as an arbitrary vector since the mathematical model is not associated with a physical system. Evidently, if the upper bound is too big and improper, it does apply a huge uncertainty to the system and the controller will fail. For example, if the states and initial conditions are on a scale of 1 or 2, the upper bound of uncertainty could be around 0.5. To have a better vision of these numbers, consider a model for an unmanned helicopter, if the mass of the system is 5(kg), the upper bound of uncertainty in the mass of the helicopter should not be more than 5+2.5(kg), 50% uncertainty in mass which can be defined as 0.5 in the modeling, which is still a huge value for uncertainty in modeling.*

The unknown parameter vector in this simulation was randomly found $\boldsymbol{\eta} = [0.2118, 0.3718, 0.1641, 0.0060]^\top$. An unknown external disturbance is set

$$w(\mathbf{x}(t), t) = \mathrm{rand}(1)\frac{4e^{-0.2t}}{1 - |x_1 - x_2|} + d_\mathrm{s}, \tag{24}$$

where rand(1) delivers a random number between $[0, 1]$ at each simulation's time-step in $t = [0, t_{\mathrm{f}}]$, and $d_{\mathrm{s}} = 0.5$ is a shift value for the disturbance. A similar discussion could be argued for the bound of disturbance as Remark 3. Based on the applied disturbance, the steady-state value is defined as $w_{\mathrm{b}} = d_{\mathrm{s}} = 0.5$, and the upper bound is $w_{\mathrm{u}} = 4.5$.

The SDC matrices must be formed based on the upper bound of the uncertainty vector which results in:

$$\mathbf{A}(\mathbf{x}, \boldsymbol{\eta}) = \begin{bmatrix} 0 & 1+\eta_{0,3} & 0 & 0 \\ 0 & 0 & 1 & 0 \\ 0 & 0 & 0 & 1+\eta_{0,4} \\ -\eta_{0,4}(x_1^2+x_2^2)e^{-|x_1|} & -4\eta_{0,1}\sin(x_1+x_3) & -0.6-\frac{1}{1+x_3^2+x_4^2}e^{-t} & -x_1\mathrm{sign}(x_1)+\eta_{0,2}+\cos(x_4) \end{bmatrix}.$$

The control parameters are also selected as $\epsilon = 0.01$, $\mathbf{Q}_{\max} = 10 \times \mathbf{I}_{4\times 4}$, with the upper/lower saturation bound of the input signal $u_{\max,\min} = \pm 2$. The initial condition is chosen $\mathbf{x}(0) = [1.25, -1.75, 0.25, -1]^\top$ and the objective is to regulate to the equilibrium point $\mathbf{x}(t_{\mathrm{f}}) = \mathbf{0}_{4\times 1}$, and the time of simulation is $t_{\mathrm{f}} = 20(\mathrm{s})$. The simulation is performed and the state variables are plotted in Fig. 2a, all of them successfully converged to zero. The output signals of the simulation are also compared with the conventional SDRE controller to show the superiority of the robust version. The input signals of both systems are shown in Fig. 2b. The information on uncertainty and disturbance was not visible to the controllers, and the control laws considered their bounds based on the proposed approach. The errors of the robust SDRE and conventional SDRE are also illustrated in Fig. 3a, in which the conventional SDRE failed to be regulated to zero, because of the shift in the steady-state value of the disturbance. The error of the robust SDRE is found 0.0180 and the error of the conventional one is obtained 0.1761.

Remark 4. *The plot of input signals of the robust SDRE and the conventional SDRE shows similar inputs when the system reaches the steady-state value, Fig. 2b. A question might arise as to why two signals are similar while their errors of them are different, plotted in Fig. 3a. Control law* (5) *includes* $\mathbf{w}_{\mathrm{b}}$*, however, the conventional SDRE does not have this term in the input law,* $\mathbf{u}(t) = -\mathbf{R}^{-1}(\mathbf{x}(t))\mathbf{B}^\top(\mathbf{x}(t), \boldsymbol{\eta}_0)\mathbf{K}(\mathbf{x}(t), \boldsymbol{\eta}_0)\mathbf{x}(t)$*. The existence of a shift in the disturbance causes a steady-state error for the conventional SDRE and it tries to compensate it as* $t \to \infty$*. So, the steady-state value of the input for the traditional SDRE is due to the steady-state error. On the contrary, the steady-state value of the robust SDRE is due to* $\mathbf{w}_{\mathrm{b}}$*, and the error of that converges to zero. Since the comparison was done with the same* $w(\mathbf{x}(t), t)$

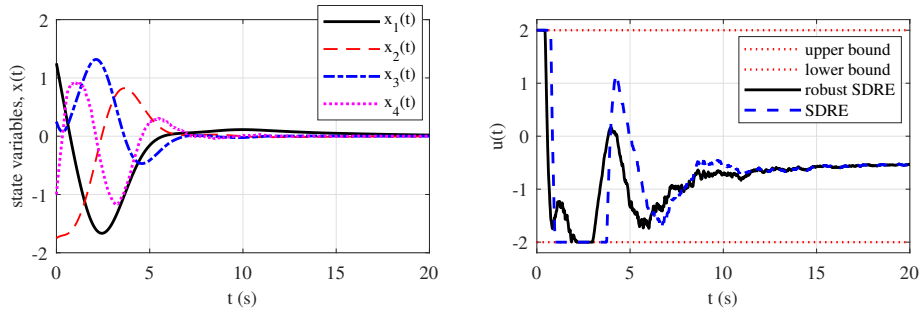

(a) The state variables. (b) The control input.

Figure 2: (a) The state variables of the system, all states regulated to zero, the equilibrium of the system. (b) The input signal, the conventional SDRE obtained a more aggressive input signal in comparison with the robust version which puts more effort into the actuators in the case of a physical model.

in (24)*, both input signals matched, however, the errors of them are different and the conventional SDRE failed.*

The traditional SDRE was unable to see the shift in the disturbance and does not have any option to handle the parameter uncertainty. The traditional SDRE is an effective method, in the domain of nonlinear optimal control and scored many applications in different fields. One of the most important aspects of the conventional SDRE is its flexible structure that can handle changes in its structure such as modified SDRE for path planning [30], combination with fuzzy [31], sliding mode control [32, 33], etc. Here in this work, another change in the structure has been shown to gain robustness.

To verify the solution with different initial conditions, a domain of $x_1(0) \in [-2, 2]$ and $x_2(0) \in [-2, 2]$ is checked for the proposed controller that resulted in the phase plane versus time, presented in Fig. 3b. The uncertainty was considered similar to the previous case $\boldsymbol{\eta} = [0.2118, 0.3718, 0.1641, 0.0060]^\top$, and the initial condition for the third and fourth states as $x_3(0) = 0.25$ and $x_4(0) = -1$. The corresponding errors at the final time were also reported in Table 1. The minimum error was found at 0.0171, the median error was 0.0190, the mean error was 0.0191, the maximum error was 0.0217, and the standard deviation was found at 0.0011. Changes in the upper bound of $\mathbf{Q}_{\max}$ also affect the error reduction. A series of simulations for various values of $\mathbf{Q}_{\max}$ is done which shows increasing the upper bound enhances the controller, presented in Fig. 4. The corresponding errors at different times

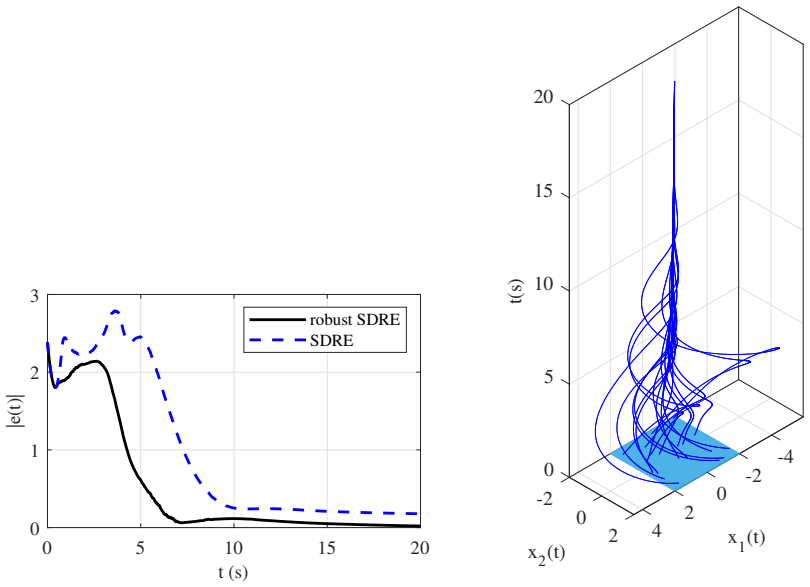

(a) The errors. (b) The phase plane.

Figure 3: (a) The error of the system in regulation, along with a comparison with conventional SDRE; in addition to the better transient performance of robust SDRE, the conventional SDRE cannot reduce the steady-state error even if the simulation time increases. (b) The phase plan for the fourth-order system with 20 different initial conditions for $x_1(0) \in [-2, 2]$ and $x_2(0) \in [-2, 2]$ for the robust SDRE controller.

were reported in Table 2 as well.

Analysis of failure: As was stated in Remark 3, an increase in the disturbance and its upper bound improperly, will fail the system to be regulated to zero. A series of analyses have been performed to study this effect briefly. Consider all the simulation parameters the same but with only a change in the upper bound of the parameter uncertainty vector $\boldsymbol{\eta}_0 = \alpha \times [0.3, 0.4, 0.2, 0.15]^\top$ and its randomly found value $\boldsymbol{\eta} = \alpha \times [0.2118, 0.3718, 0.1641, 0.0060]^\top$. If one considers different values for $\alpha = \{0.1, 0.5, 1, 1.5, 2, 2.25, 2.5\}$ as a scale for highlighting the effect of uncertainty in the simulation, for $\alpha \leq 2$ the performance of the controller is acceptable. For $\alpha = 2.25, 2.5$, and more, the controller failed to regulate the system to the equilibrium point, see Fig. 5.

Table 1: The error of the system at the final time with respect to the different initial conditions; 20 randomly chosen values in the domain of $x_1(0) \in [-2, 2]$ and $x_2(0) \in [-2, 2]$ were simulated.

No.	$x_1(0)$	$x_2(0)$	$e(20)$
1	1.61911	1.578828	0.017058
2	1.438366	-1.33313	0.02168
3	-0.39209	1.754473	0.018378
4	0.945881	0.936684	0.018501
5	1.617914	-1.48369	0.018367
6	1.834861	1.284406	0.018509
7	-1.15196	-0.8757	0.019748
8	0.823012	0.301953	0.019717
9	-1.46334	1.518763	0.017593
10	-0.45826	-0.27979	0.019049
11	-0.71128	-1.24605	0.018878
12	-0.58746	0.795487	0.01873
13	1.423481	-1.47013	0.018566
14	-0.5057	-1.90257	0.019146
15	1.590355	-1.32696	0.020772
16	-0.95428	1.076854	0.020045
17	-0.33583	1.531081	0.020185
18	-0.16811	-0.48931	0.01958
19	0.447787	1.669265	0.019033
20	-0.25368	-0.30394	0.019204

4. Comparison and Analysis

This section presents a comparison between the proposed robust control design and conventional ones. Sliding mode control is a well-established and effective controller in the domain of robust control, which is selected as a candidate for comparison. The system for simulation is a disturbed uncertain Van der Pol equation subjected to forced control input for regulation to equilibrium point $\mathbf{x}_{\text{des}} = \mathbf{0}$:

$$\dot{\mathbf{x}}(t) = \begin{bmatrix} 0 & 1+\eta_1 \\ -1 & \eta_2(1-x_1^2(t)) \end{bmatrix} \mathbf{x}(t) + \begin{bmatrix} 0 \\ 1 \end{bmatrix} (u(t) + w(\mathbf{x}(t), t)),$$

where $w(\mathbf{x}(t), t)$ is set as Eq. (24), and $\boldsymbol{\eta} = \text{diag}(\text{rand}(2, 1))\boldsymbol{\eta}_0$, in which the upper bound is $\boldsymbol{\eta}_0 = [0.2, 0.4]^\top$. The upper bound of uncertainty generates

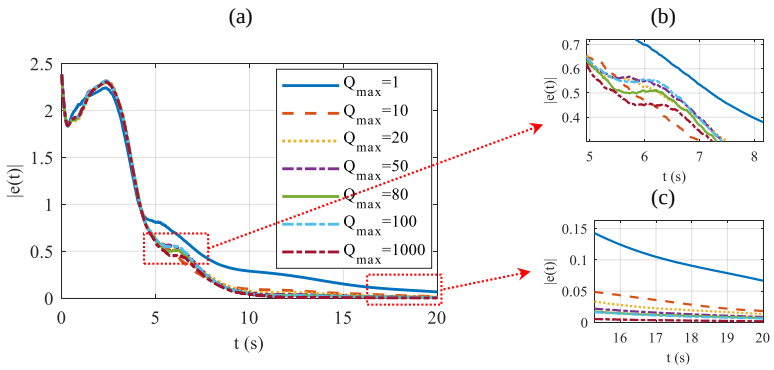

Figure 4: The effect of the upper bound of $\mathbf{Q}(\mathbf{x})$ matrix on the error reduction; (a) error reduction in the entire time domain, (b) a zoomed-view around 6(s) of simulation, (c) a zoomed view at the end of simulation 14-20(s).

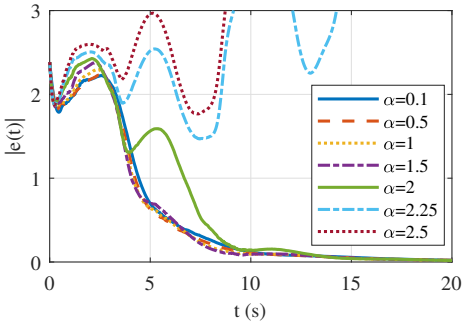

Figure 5: The effect of disturbance and analysis of failure; $\alpha > 2$ failed as it imposed a huge uncertainty on the system, please revisit Remark 3.

the nominal SDC matrix $\mathbf{A}(\mathbf{x}, \boldsymbol{\eta}_0) = \begin{bmatrix} 0 & 1+\eta_{0,1} \\ -1 & \eta_{0,2}(1-x_1^2(t)) \end{bmatrix}$.

The steady-state value of the disturbance is $w_{\text{b}} = 0.5$, the upper bound of that is $w_{\text{u}} = 4.5$, and $\epsilon = 0.01$. The maximum bound of weighting matrix is $\mathbf{Q}_{\max} = 10 \times \mathbf{I}_{2\times 2}$, weighting value of the input is $R_{\min} = \epsilon$ and the control input of the system is limited by $u_{\max,\min} = \pm 2$.

The classical sliding mode control, an effective approach in robust design, is chosen for comparison. The sliding surface is set as $s(\mathbf{x}(t)) = \dot{e}(t) + \lambda e(t)$ where $e(t) = x_1(t) - x_{\text{des},1}$, $\dot{e}(t) = x_2(t) - x_{\text{des},2}$ and $\lambda > 0$ is a strictly positive

Table 2: The role of the upper bound of $\mathbf{Q}(\mathbf{x}(t))$ on the error reduction; increasing the value of $\mathbf{Q}_{\max}$ reduces the error and the produced graphs in Fig. 4 would be similar to $\mathbf{Q}_{\max} = 1000$.

No.	$\mathbf{Q}_{\max}$	$e(10)$	$e(15)$	$e(20)$
1	1	0.33212	0.136727	0.065795
2	10	0.091924	0.050451	0.01982
3	20	0.064916	0.036398	0.013243
4	50	0.050676	0.023252	0.009211
5	80	0.047126	0.020482	0.006621
6	100	0.03986	0.016851	0.006089
7	1000	0.048411	0.006318	0.00205

constant. The control law is in the form of

$$u_{\text{SMC}}(t) = -f(\mathbf{x}(t)) - k_{\text{SMC}}\ \text{sign}(s(\mathbf{x}(t))),$$

where $f(\mathbf{x}(t)) = -x_1(t) + \eta_{0,2}(1 - x_1^2(t))x_2(t)$. The initial condition of the simulation is chosen $\mathbf{x}(0) = [-1, 1.5]^\top$, $\lambda = 1$ and $k_{\text{SMC}} = 2$, and time of simulation is set $t_{\text{f}} = 20$(s). The phase plane of the system in the simulation is shown in Fig. 6a. The input signals of the three methods are also illustrated in Fig. 6b. The regulation error for the conventional SDRE was gained 0.1651, SMC 0.0361, and the robust SDRE 0.0145. The close result of the SMC to the proposed robust SDRE was gained with the cost of chattering and bigger input signal, presented in Fig. 6b. In order to remove the chattering, typical treatments such as using "arctan" function was considered and simulated to enhance the performance. Increase in the gains $\lambda = 2$ and $k_{\text{SMC}} = 10$ resulted in error of SMC 0.0272, but without chattering. The states and inputs are illustrated in Figs. 7a and 7b, respectively. This comparison was done to show that the performance of the proposed robust design is acceptable. Clearly, the sliding mode control with tuning and iterations might get closer results to optimal robust SDRE controller.

The sensitivity of the performance of the proposed design is checked in terms of different external disturbance functions. The error of the system has been computed as an index in response to them in the regulation case, presented in this section. The disturbance function Eq. (24) is bounded based on Assumption 1 though it has a steady-state shift which is difficult to handle via conventional SDRE. Sliding mode control handled the shift using the

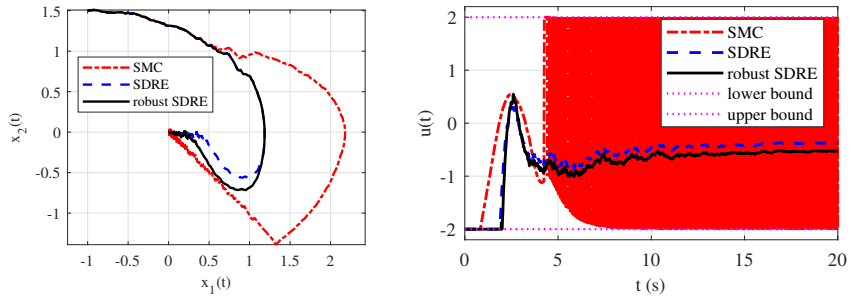

(a) The phase plane. (b) The control input.

Figure 6: The simulation of the Van der Pol oscillator using the "sign" function.

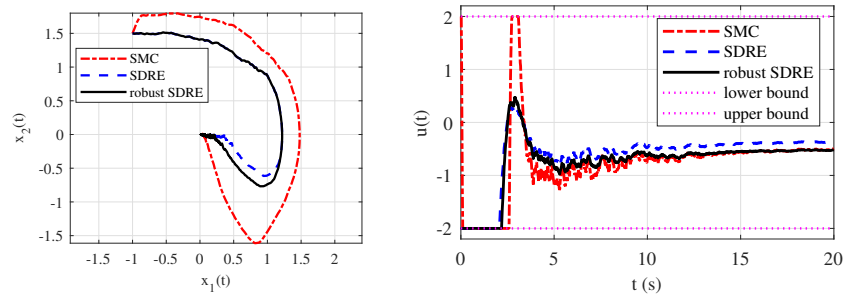

(a) The phase plane. (b) The control input.

Figure 7: The simulation of the Van der Pol oscillator using the "atan" function.

correction part of the control law $k_{\text{SMC}}\ \text{sign}(s(\mathbf{x}(t)))$ or $k_{\text{SMC}}\ \arctan(s(\mathbf{x}(t)))$. Here a series of disturbance functions is simulated and the results are reported in Table 3. The control parameters and simulation condition are based on Section 4 and SMC with the "arctan" function. The amplitude of disturbance requires tuning though without that, the proposed design gained less root-mean-square error at the final time for the various types of external disturbance, see Table 3.

5. Conclusions

This work presented a robust state-dependent Riccati equation controller for nonlinear systems with mismatched parameter uncertainty and matched disturbance. The disturbance has a steady-state shift and it will not tend

Table 3: The sensitivity of the error in the regulation of the Van der Pol equation subjected to different disturbance types. RMS stands for root mean square.

No.	disturbance $w(\mathbf{x}(t), t)$	RMS($e(t_\mathrm{f})$) SDRE	RMS($e(t_\mathrm{f})$) SMC	RMS($e(t_\mathrm{f})$) robust SDRE
1	$\mathrm{rand}(1)\frac{4e^{-0.2t}}{1-\lvert x_1-x_2\rvert}+d_\mathrm{s}$	0.1631	0.0268	0.0128
2	$\mathrm{rand}(1)\frac{4e^{-0.2t}}{1-\lvert x_1-x_2\rvert}-d_\mathrm{s}$	0.1376	0.0230	0.0131
3	d_s	0.1508	0.0250	8.4946×10^{-12}
4	$\mathrm{rand}(1)\times0.1\times(t_\mathrm{f}-t)+d_\mathrm{s}$	0.1685	0.0261	0.0221
5	$4\times\mathrm{rand}(1)+d_\mathrm{s}$	0.7214	0.6809	0.5734

to zero when time goes to infinity. This made it impossible for the conventional SDRE to regulate the system to zero since it only works with systems with zero equilibrium points. The mentioned case and also the sensitivity of the conventional SDRE to uncertainty in modeling motivated this work to present a robust structure for the SDRE, using its own capability and design flexibility. The stability of the robust SDRE was presented (based on the second Lyapunov stability criteria) and delivered two tuning rules for the selection of weighting matrices to gain stability in transient and steady-state conditions. The analytical proof of stability was presented for the robust design. Those obtained tuning conditions were found under the umbrella of the SDRE without combining the method with other tools such as neural networks, fuzzy, or other apparatus. A fourth-order differential equation was selected as an example for the simulation study. The simulation results confirmed the effectiveness of the controller and outperformed the conventional SDRE. The changes in the parameters, the effect of uncertainty on the failure, bounds, etc. have been investigated to clarify to performance of the proposed structure.

Proposal for future study: This proposed design revealed the implementation of a robust method based on the state-dependent Riccati equation as a unified method within the framework of nonlinear optimal control. The application of this method could be developed for various systems such as flapping-wing flying robots (FWFRs) which inherit complicated hybrid and disturbed dynamics [34]. The uncertainty is rooted in the equivalence of flapping and the base excitation model. Flapping itself also exerts a periodic excitation as a disturbance to the body of the base. Hence this method

could be a good option to handle the uncertain and disturbed dynamics of FWFR and enhance the control performance. From the theoretical point of view, the tracking case could be developed for the same concept through the implementation of stationary and necessary conditions for optimality on the Hamiltonian which includes the tracking error inside the cost function. Following the difference between the regulation (current work) [35], and tracking problem [36], the mentioned references could be visited and the derivation method could be applied considering the uncertainty and disturbance in the system and cost function.

CRediT authorship contribution statement

S. R. Nekoo: Methodology, Investigation, Formal analysis, Coding and Programming, Writing – original draft, Writing - review & editing. Anibal Ollero: Supervision, Project administration, Funding acquisition, Resources, Writing – review & editing.

Conflict of interest

There is not any conflict of interest reported by the authors.

Acknowledgements

This work was supported by the European Project GRIFFIN ERC Advanced Grant 2017, Action 788247, and by the European Commission H2020 Program AERIAL-CORE, contract No. 871479.

Data availability

The MATLAB codes of the simulations of this paper will be publicly available on the MATLAB Central website and as supplementary material on the journal's website.

References

[1] J. Pearson, Approximation methods in optimal control I. Sub-optimal control, International Journal of Electronics 13 (5) (1962) 453–469.

[2] T. Çimen, Approximate nonlinear optimal SDRE tracking control, in: 17th IFAC Symp. Automatic Control in Aerospace, Vol. 40(7), Elsevier, 2007, pp. 147–152.

[3] T. Cimen, Survey of state-dependent Riccati equation in nonlinear optimal feedback control synthesis, Journal of Guidance, Control, and Dynamics 35 (4) (2012) 1025–1047.

[4] J. R. Cloutier, State-dependent Riccati equation techniques: An overview, in: Proceedings of the 1997 American control conference (Cat. No. 97CH36041), Vol. 2, IEEE, 1997, pp. 932–936.

[5] M. Nazari, N. Babaei, M. Nazari, Nonlinear SDRE based adaptive fuzzy control approach for age-specific drug delivery in mixed chemotherapy and immunotherapy, Biomedical Signal Processing and Control 68 (2021) 102687.

[6] S.-W. Kim, S.-Y. Park, C. Park, Spacecraft attitude control using neuro-fuzzy approximation of the optimal controllers, Advances in Space Research 57 (1) (2016) 137–152.

[7] S. Ozcan, E. H. Copur, A. C. Arican, M. U. Salamci, A modified SDRE-based sub-optimal hypersurface design in SMC, IFAC-PapersOnLine 53 (2) (2020) 6250–6255.

[8] M. Habibnejad Korayem, N. Ghobadi, S. Fathollahi Dehkordi, Designing an optimal control strategy for a mobile manipulator and its application by considering the effect of uncertainties and wheel slipping, Optimal Control Applications and Methods 42 (5) (2021) 1487–1511.

[9] R. F. da Costa, O. Saotome, E. Rafikova, R. Machado, Fast real-time SDRE controllers using neural networks, ISA transactions 118 (2021) 133–143.

[10] J. Lee, Y. Lee, Y. Kim, G. Moon, B.-E. Jun, Design of an adaptive missile autopilot considering the boost phase using the SDRE method and neural networks, Journal of the Franklin Institute 355 (18) (2018) 9085–9107.

[11] S. R. Nekoo, Tutorial and review on the state-dependent Riccati equation, Journal of Applied Nonlinear Dynamics 8 (2) (2019) 109–166.

[12] J. R. Cloutier, C. N. D'Souza, C. P. Mracek, Nonlinear regulation and nonlinear H_∞ control via the state-dependent riccati equation technique: Part 1, theory, in: Proceedings of the international conference on nonlinear problems in aviation and aerospace, Embry Riddle University, 1996, pp. 117–131.

[13] K. A. Wise, J. L. Sedwick, Nonlinear control of agile missiles using state dependent Riccati equations, in: Proceedings of the 1997 American Control Conference (Cat. No. 97CH36041), Vol. 1, IEEE, 1997, pp. 379–380.

[14] N. Nasiri, A. Fakharian, M. B. Menhaj, A novel controller for nonlinear uncertain systems using a combination of SDRE and function approximation technique: Regulation and tracking of flexible-joint manipulators, Journal of the Franklin Institute 358 (10) (2021) 5185–5212.

[15] L. Roveda, D. Piga, Robust state dependent Riccati equation variable impedance control for robotic force-tracking tasks, International Journal of Intelligent Robotics and Applications 4 (4) (2020) 507–519.

[16] S. R. Kumar, A. Maity, Finite-horizon robust suboptimal control-based impact angle guidance, IEEE Transactions on Aerospace and Electronic Systems 56 (3) (2019) 1955–1965.

[17] S. R. Nekoo, Digital implementation of a continuous-time nonlinear optimal controller: An experimental study with real-time computations, ISA transactions 101 (2020) 346–357.

[18] L. Hou, L. Wang, H. Wang, Smc for systems with matched and mismatched uncertainties and disturbances based on NDOB, Acta Automatica Sinica 43 (7) (2017) 1257–1264.

[19] H. Wang, J. Wang, X. Chen, K. Shi, H. Shen, Adaptive sliding mode control for persistent dwell-time switched nonlinear systems with matched/mismatched uncertainties and its application, Journal of the Franklin Institute 359 (2) (2022) 967–980.

[20] Y. Kim, S. Kwon, Robust stabilization of underactuated two-wheeled balancing vehicles on uncertain terrains with nonlinear-model-based disturbance compensation, in: Actuators, Vol. 11(11), MDPI, 2022, p. 339.

[21] H. R. Shafei, M. Bahrami, Trajectory tracking control of a wheeled mobile robot in the presence of matched uncertainties via a composite control approach, Asian Journal of Control 23 (6) (2021) 2805–2823.

[22] M. Khoshhal Rudposhti, M. A. Nekoui, M. Teshnehlab, Robust optimal control for a class of nonlinear systems with uncertainties and external disturbances based on SDRE, Cogent Engineering 5 (1) (2018) 1451014.

[23] N. Nasiri, A. Fakharian, M. B. Menhaj, Observer-based robust control for flexible-joint robot manipulators: A state-dependent Riccati equation-based approach, Transactions of the Institute of Measurement and Control 42 (16) (2020) 3135–3155.

[24] Y.-L. Kuo, Robust chaos synchronizations using an SDRE-based suboptimal control approach, Nonlinear Dynamics 76 (1) (2014) 733–742.

[25] N. Le-Dung, P. Huynh-Lam, N. Hoang-Giap, N. Tan-Luy, Event-triggered distributed robust optimal control of nonholonomic mobile agents with obstacle avoidance formation, input constraints and external disturbances, Journal of the Franklin Institute 360 (8) (2023) 5564–5587.

[26] S. Xiong, H. H.-T. Liu, Low-altitude fixed-wing robust and optimal control using a barrier penalty function method, Journal of Guidance, Control, and Dynamics (2023) 1–6.

[27] Y. Qiu, Y. Li, Y. Liu, Z. Wang, K. Liu, Observer-based robust optimal control for helicopter with uncertainties and disturbances, Asian Journal of Control (2023).

[28] S. Yang, G. Tao, B. Jiang, Robust adaptive control of nonlinearly parametrized multivariable systems with unmatched disturbances, International Journal of Robust and Nonlinear Control 30 (9) (2020) 3582–3606.

[29] S. Yang, G. Tao, B. Jiang, Y. Zhang, W. Lin, Modeling and adaptive control of air vehicles with partial nonlinear parametrization, Automatica 149 (2023) 110805.

[30] M. H. Korayem, S. R. Nekoo, The SDRE control of mobile base cooperative manipulators: Collision free path planning and moving obstacle avoidance, Robotics and Autonomous Systems 86 (2016) 86–105.

[31] M. Abdelrahman, S.-Y. Park, Spacecraft attitude control via a combined state-dependent Riccati equation and adaptive neuro-fuzzy approach, Aerospace Science and Technology 26 (1) (2013) 16–28.

[32] Y.-W. Liang, Y.-T. Wei, D.-C. Liaw, C.-C. Cheng, L.-G. Lin, A study of SDRE and ISMC combined scheme with application to vehicle brake control, in: Proceedings of SICE Annual Conference 2010, IEEE, 2010, pp. 497–502.

[33] A. H. Korayem, S. R. Nekoo, M. Korayem, Sliding mode control design based on the state-dependent Riccati equation: theoretical and experimental implementation, International Journal of Control 92 (9) (2019) 2136–2149.

[34] S. R. Nekoo, A. Ollero, Closed-loop nonlinear optimal control design for flapping-wing flying robot (1.6 m wingspan) in indoor confined space: Prototyping, modeling, simulation, and experiment, ISA transactions (2023).

[35] M. H. Korayem, S. Nekoo, Finite-time state-dependent Riccati equation for time-varying nonaffine systems: Rigid and flexible joint manipulator control, ISA transactions 54 (2015) 125–144.

[36] M. H. Korayem, S. Nekoo, State-dependent differential Riccati equation to track control of time-varying systems with state and control nonlinearities, ISA transactions 57 (2015) 117–135.